Journal of Chemical&Engineering Data

pubs.acs.org/jced Article

Comprehensive Physicochemical Investigation of the Water-Soluble Adduct of C_{60} with L-Methionine ($C_{60}(C_5H_{11}NO_2S)_3$): Important Data for Further Applications

Konstantin N. Semenov,* Ali Mlhem, Alexander V. Akentiev, Dmitry A. Nerukh, Natalia V. Petukhova, Ilnaz T. Rakipov, Kirill V. Timoshchuk, Gleb O. Iurev, Andrey V. Petrov, Igor V. Murin, Nikolay A. Charykov, Olga S. Vezo, Anastasia V. Penkova, Dilafruz K. Kholmurodova, Jasur A. Rizaev, Aziz S. Kubaev, and Vladimir V. Sharoyko*

Cite This: https://doi.org/10.1021/acs.jced.5c00146 Read Online

ACCESS | Metrics & More | Article Recommendations | Supporting Information

ABSTRACT: This work is devoted to the study of the physicochemical properties of the water-soluble adduct fullerene C_{60}-L-methionine. The adduct was characterized using ^{13}C solid-state NMR spectroscopy, IR spectroscopy, elemental analysis, UV/vis spectroscopy, and HPLC. The measured physicochemical properties included density, viscosity, refraction, electrical conductivity, speed of sound, surface properties of aqueous solutions, nanoparticle size distribution in water, the molecular dynamics simulation of the association of C_{60}-Met molecules in water and isotonic saline (0.15 M NaCl solutions), the study of solubility in binary C_{60}-Met−H_2O and ternary C_{60}-Met−NaCl−H_2O systems, as well as their distribution in the *n*-octan-1-ol−water system.

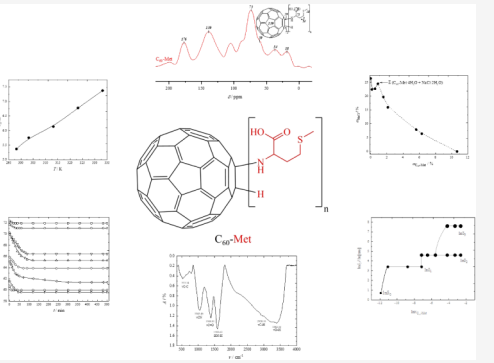

1. INTRODUCTION

Fullerenes have unique properties for application in various fields of science and technology, such as biology, medicine, bioanalytics, materials science, nanotechnology, etc.[1,2] Fullerenes, due to their pronounced biological activity, have great potential for medicine, but a major obstacle is their low solubility in aqueous solutions.[3,4] Synthetic approaches developed in recent years for obtaining water-soluble fullerene adducts (polyhydroxylated fullerenes, carboxylated fullerenes, fullerene adducts with amino acids and peptides) are a substantial achievement in the chemistry of fullerenes.[1,2,5−8] The potential of these compounds is associated with a wide range of their biological activities. Literature analysis shows that fullerene adducts possess antitumor, antiviral, antibacterial, antioxidant, and neuroprotective properties, as well as photodynamic and membranotropic activity.[9−11] Obviously, the physicochemical properties of solutions of biologically active compounds form the basis of understanding their mechanism of action, as well as pharmacokinetics, pharmacodynamics, and metabolic stability, which makes it possible to evaluate intermolecular interactions in solution, hemocompatibility, permeability through tissue barriers, etc. It is also well known that the size of nanoparticles determines their bioavailability, toxicity, and mechanism of action.[12−27]

The analysis of the literature on various water-soluble fullerene adducts shows that, to date, the physical chemistry of amino acid and peptide fullerene adducts has been studied, such as the thermodynamic properties of solids, phase equilibria, and physicochemical properties of solutions. Computer modeling was used for investigating the mechanisms of adduct association, the energetics of the interaction of individual fullerenes with amino acids and peptides, as well as the properties of their solutions. Andreeva et al.[28] calculated the Gibbs free energy, enthalpy, and entropy changes in the formation of amino ($C_{60}H_n(NH_2)_n$) and carboxamide ($C_{60}H_n(NH_2)_n(CO_2)_n$) derivatives of fullerene C_{60}. It was shown that the formation of carboxamide derivatives is determined by the enthalpy factor and that these adducts are also prone to cluster formation in aqueous solutions. Luzhkov et al. obtained the values of the dissociation constants of the adduct of C_{60} with L-alanine, which were pK_D (−NH) = −1.44, pK_D (−COOH) = 4.2, and pK_D (−CH−) = 5.8.[29] Basiuk et al. calculated the energy of complex formation of glycine and L-alanine oligopeptides with C_{60} using DFT and molecular mechanics methods (GGA-BLYP and LDA-VWN functionals, and AMBER, MM+ force fields).[30] The

Received: March 6, 2025
Revised: July 23, 2025
Accepted: August 1, 2025

physicochemical properties of fullerene adduct solutions were also investigated. The authors of references[31−39] studied adducts of light fullerenes with proteinogenic amino acids and dipeptides. In particular, they studied the refractive index, heat capacity, density, viscosity, electrical conductivity, size distribution of associates, and the excess thermodynamic functions of solutions at various concentrations and temperatures. In references[35,36,39], the phase equilibria in binary systems C_{60}-Arg−H_2O, C_{60}−Thr−H_2O, C_{60}-Lys−H_2O, and the ternary system C_{60}-Lys−NaCl−H_2O were studied. The results led to the following conclusions: (*i*) water-soluble adducts of fullerenes with amino acids in dilute solutions usually have negative and large absolute values of partial molar volumes, which indicates the compaction and structuring of solutions; (*ii*) the works[33,35,40] show that water-soluble fullerene adducts are weak electrolytes; (*iii*) it was established that fullerene adducts with amino acids in aqueous solutions are strongly associated;[33,41] and (*iv*) the synthesized fullerene adducts with amino acids and peptides are well soluble in water and aqueous solutions.[1,33,34,40,41]

This work is devoted to the study of the physicochemical properties of the water-soluble C_{60}-L-methionine adduct (C_{60}-Met, $C_{60}(C_5H_{11}NO_2S)_3$). The adduct was characterized using ^{13}C solid-state NMR spectroscopy, IR spectroscopy, elemental analysis, UV/vis spectroscopy, and HPLC. Density, viscosity, refractive index, electrical conductivity, the speed of sound, surface properties of aqueous solutions, and nanoparticle size distribution in water were measured. Molecular dynamics computer simulation of C_{60}-Met association in pure water and isotonic saline (0.15 M NaCl) was carried out. The study of solubility in binary C_{60}-Met−H_2O and ternary C_{60}-Met−NaCl−H_2O systems, as well as the distribution in the *n*-octan-1-ol−water system, was performed.

2. EXPERIMENTAL AND COMPUTATIONAL METHODS

2.1. Materials. The C_{60}-Met was purchased from "MST Nano", St. Petersburg; *n*-octan-1-ol sample was purchased from Sigma−Aldrich. The samples were used without further purification, and we did not perform the separation of positional isomers of C_{60}-Met. The characteristics of the samples are indicated in Table 1.

Table 1. Characteristics of the Chemical Samples

Name	Supplier	Purity, kg·kg^{-1}	Analysis method
n-octan-1-ol	Sigma-Aldrich	>0.985	Gas chromatography
C_{60}-Met	MST Nano	>0.995	Liquid chromatography

Deionized water was used (electrical conductivity equal to 5.6 × 10^{-6} S·m^{-1}). Purification of water was performed using a Millipore Simplicity UV apparatus (Merck KGaA, Germany). Aqueous solutions of C_{60}-Met were prepared by mixing the components in different proportions by mass using an electronic balance with an uncertainty of ±0.0001 g. The solutions were stored in airtight, glass-stoppered bottles to prevent contamination and evaporation.

All uncertainties were estimated according to the Guide to the Expression of Uncertainty in Measurement (GUM).[42]

2.2. C_{60}-Met Characterization. To characterize the C_{60}-Met adduct, a group of physicochemical methods was used. A detailed description of the equipment is given in Table S1. The characterization of C_{60}-Met is presented in Figures S1−S4.

2.3. Physicochemical Investigation. Density, refraction, viscosity, electrical conductivity, speed of sound, and surface properties of C_{60}−Met aqueous solutions were analyzed according to the methods described in references[32,34−36,39,41,43−49]. The density measurements were carried out using a DMA 5000 M density meter (Anton Paar, Austria). The viscosity of the investigated samples was measured using a Lovis 2000 M rolling-ball microviscometer (Anton Paar, Austria). The refractive indices of the solutions were determined using an Abbemat WR-MW automatic refractometer (Anton Paar, Austria). Electrical conductivity was measured using an Anion-4151 (NV-Lab, Russia). Speed of sound measurements were carried out using a DSA 5000 (Anton Paar, Austria). Surface properties were investigated using a Spectra apparatus (Ntegra, Russia) and Sigma 701 (Biolin Scientific, Finland). The size distribution of C_{60}-Met associates in aqueous solutions and their electrophoretic mobility were measured using a Zetasizer apparatus (Malvern, UK).

The methodology for studying the association of C_{60}-Met in water and isotonic saline (0.15 M NaCl) using the Molecular Dynamics (MD) method is described in Supporting materials.

To study the nature of the C_{60}-Met association at the atomic-molecular level, quantum chemistry and MD were used. The electronic structure of C_{60}-Met was calculated in the ORCA program using the DFT method, CAM-B3LYP 6−31g* functional, and atomic basis set, with full geometry optimization and taking into account the interaction with the solvent according to the CPCM model. The choice of the functional and basis set was based on the successful application of this scheme for predicting electronic absorption spectra. The association of C_{60}-Met in water and isotonic saline (0.15 M NaCl) was studied by MD. The atomic charges, estimated according to the Mulliken scheme, were used from quantum chemical calculations. The GROMACS 2023 package was used for molecular dynamics calculations. For calculations with periodic boundary conditions, 20 C_{60}-Met molecules and 1.3 × 10^5 water molecules were placed in a cubic cell with sides of 16 nm; the distance between the C_{60}-Met molecules was 30 Å, the distance from the C_{60}-Met molecule to the cell edge was 15 Å, and the diameter of the C_{60}-Met molecule was 15−20 Å. The OPLS-AA/M force field was used for the calculations; the simulation time was 400 ns with a step of 1 fs. Next, in the GROMACS 2023 package, solvation, energy minimization, and equilibration of the system were carried out in the NVT and NPT ensembles with a thermostat and Berendsen barostat for 400 ps with a time step of 0.1 fs under the conditions T = 298.15 K and p = 101325 Pa.

The solubility in the C_{60}-Met−H_2O binary system was studied by isothermal saturation in ampules at temperatures ranging from 298.15 to 333.15 K, as described in ref.50. The same procedure was used for the investigation of solubility in the C_{60}-Met−NaCl−H_2O ternary system at 298.15 K.

The detailed methodology for determining the coefficient of the distribution of C_{60}-Met in the *n*-octan-1-ol−water system is presented in ref.50.

3. RESULTS AND DISCUSSION

3.1. Physicochemical Investigation of C_{60}-Met. *3.1.1. Densities and Volume Properties of C_{60}-Met Water Solutions.* Table 2 and Figure S5 present T−C data on solution densities. The analysis of Figure S5 shows that the density values rise with the increase in concentration of C_{60}-Met.

https://doi.org/10.1021/acs.jced.5c00146
J. Chem. Eng. Data XXXX, XXX, XXX−XXX

Table 2. Temperature (T) and Concentration (C) Dependences of Density (ρ) of C_{60}-Met Aqueous Solutions at p = 0.1 MPa[a]

$x_{C60\text{-}Met}$	T/K					
	283.15	293.15	303.15	313.15	323.15	333.15
			ρ/kg·m^{-3}			
1.55×10^{-7}	999.78	998.30	995.75	992.32	988.12	983.27
4.64×10^{-7}	999.80	998.31	995.76	992.33	988.14	983.29
7.73×10^{-7}	999.81	998.34	995.79	992.34	988.17	983.32
1.55×10^{-6}	999.85	998.37	995.81	992.38	988.18	983.36
4.64×10^{-6}	999.99	998.51	995.95	992.53	988.33	983.49
7.73×10^{-6}	1000.14	998.65	996.10	992.67	988.47	983.63
1.55×10^{-5}	1000.44	998.95	996.38	992.95	988.76	983.91
4.64×10^{-5}	1001.62	1000.10	997.52	994.08	989.88	985.01
7.73×10^{-5}	1002.80	1001.26	998.67	995.21	991.00	986.12
1.08×10^{-4}	1003.96	1002.41	999.80	996.34	992.11	987.26
1.54×10^{-4}	1005.68	1004.10	1001.47	997.98	993.75	988.89

[a][a]Standard uncertainty is $u(T)$ = 0.01 K, $u(P)$ = 10 kPa. Combined expanded uncertainty for ρ is $Uc(\rho)$ = 0.01 kg·m^{-3} (0.95 level of confidence).

Table 3. Refraction Properties of C_{60}-Met Aqueous Solutions in Water at T = 293.15 K. C is the Volume Concentration of C_{60}-Met, n_D is the Refraction Index; R and R are Specific and Molar Refractions, $r_{C_{60}-Met}$ and $R_{C_{60}-Met}$ are Specific and Molar Refractions of C_{60}-Met Aqueous Solutions at λ = 589.3 nm and p = 0.1 MPa[a]

$x_{C_{60}-Met}$	n_D	$r/10^{-4}$·m^3·kg^{-1}	$R/10^{-6}$ m^3·mol^{-1}	$R_{C_{60}-Met}/10^{-4}$·m^3·mol^{-1}	$r_{C_{60}-Met}/10^{-4}$·m^3·kg^{-1}
1.55×10^{-7}	1.33302	2.0607	3.7092	—	—
4.64×10^{-7}	1.33045	2.0607	3.7093	—	—
7.73×10^{-7}	1.33304	2.0606	3.7094	—	—
1.55×10^{-6}	1.33312	2.0606	3.7096	3.1684	2.7664
4.64×10^{-6}	1.33315	2.0608	3.7104	3.0677	2.6287
7.73×10^{-6}	1.33328	2.0609	3.7112	2.8806	2.4685
1.55×10^{-5}	1.33332	2.0610	3.7134	2.8637	2.4539
4.64×10^{-5}	1.33385	2.0615	3.7216	2.7635	2.3681
7.73×10^{-5}	1.33441	2.0622	3.7301	2.7721	2.3754
1.08×10^{-4}	1.33492	2.0628	3.7385	2.7681	2.3721
1.54×10^{-4}	1.33576	2.0635	3.7511	2.7560	2.3616

[a][a]Standard uncertainties are $u(T)$ = 0.03 K, $u(P)$ = 10 kPa, and $u(n_D)$ = 0.00004 (0.95 level of confidence).

Table 4. Temperature and Concentration Dependences of Dynamic (η) and Kinematic (η_k) Viscosities of C_{60}-Met Aqueous Solutions[ab]

$x_{C_{60}-Met}$	T/K						T/K					
	283.15	293.15	303.15	313.15	323.15	333.15	283.15	293.15	303.15	313.15		
	η /mPa·s						η_k /mm^2 ·s^{-1}					
1.55×10^{-7}	1.306	1.002	0.799	0.656	0.553	0.476	1.306	1.004	0.802	0.661	0.559	0.484
4.64×10^{-7}	1.307	1.003	0.799	0.657	0.553	0.476	1.308	1.005	0.803	0.662	0.560	0.484
7.73×10^{-7}	1.307	1.003	0.799	0.657	0.553	0.476	1.308	1.005	0.803	0.662	0.560	0.484
1.55×10^{-6}	1.307	1.003	0.800	0.657	0.553	0.476	1.307	1.005	0.803	0.662	0.560	0.484
4.64×10^{-6}	1.310	1.005	0.801	0.658	0.555	0.477	1.310	1.007	0.805	0.663	0.561	0.485
7.73×10^{-6}	1.312	1.006	0.802	0.659	0.555	0.478	1.311	1.008	0.805	0.664	0.561	0.486
1.55×10^{-5}	1.317	1.010	0.805	0.661	0.557	0.479	1.316	1.011	0.808	0.666	0.563	0.487
$4.64 \times \times 10^{-5}$	1.334	1.024	0.816	0.671	0.565	0.486	1.332	1.024	0.818	0.675	0.571	0.493
7.73×10^{-5}	1.354	1.039	0.828	0.679	0.572	0.491	1.350	1.038	0.829	0.683	0.577	0.498
1.08×10^{-4}	1.374	1.055	0.841	0.69	0.581	0.497	1.369	1.052	0.841	0.692	0.585	0.504
1.54×10^{-4}	1.402	1.075	0.856	0.703	0.591	0.507	1.394	1.071	0.855	0.704	0.594	0.512

[a]C is the volume concentration of C_{60}–Met in aqueous solution at p = 0.1 MPa. [b]Standard uncertainties are $u(T)$ = 0.02 K, $u(P)$ = 10 kPa, and $u_r(\eta)$ = 1% (0.95 level of confidence).

The average molar volumes (V) of solutions were calculated using eq 1:

$$\overline{V} = V/(n_1 + n_2) \quad (1)$$

where the summation is carried out for both components (1 is H_2O, 2 is C_{60}–Met). V and n_i are the volume and the number of moles of the *ith* component in one liter of solution. The average molar volumes are presented in Figure S6.

The calculation of the partial molar volumes of solution components V_i was carried out according to eqs 2 and 3:

$$V_{H_2O} = \overline{V} - x_{C_{60}-Met} \cdot (\partial \overline{V}/\partial x_{C_{60}-Met})_{T,P} \quad (2)$$

https://doi.org/10.1021/acs.jced.5c00146
J. Chem. Eng. Data XXXX, XXX, XXX−XXX

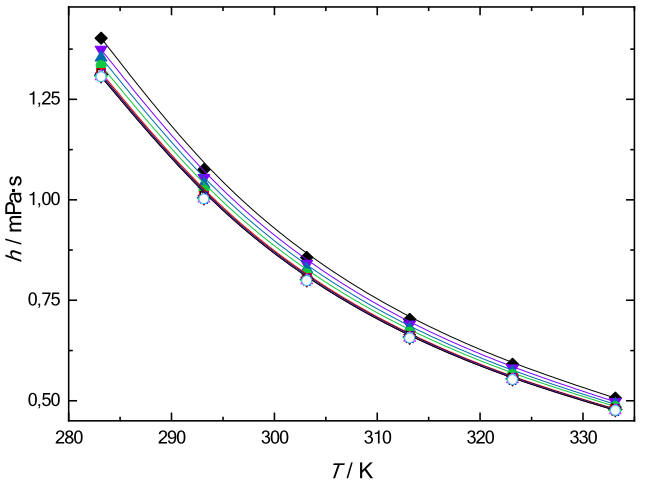

Figure 1. Temperature dependences (T) of dynamic viscosity (η) of C_{60}-Met aqueous solutions at different concentrations ($x_{C_{60}-Met}$): (**orange square**) 0, (**blue circle**) 1.55×10^{-7}, (**pink triangle**) 4.64×10^{-7}, (**brown inverted triangle**) 7.73×10^{-7}, (**green rhombus**) 1.55×10^{-6}, (blue left-tilted triangle) 4.64×10^{-6}, (brown right-tilted triangle) 7.73×10^{-6}, (red square) 1.55×10^{-5}, (green small circle) 4.64×10^{-5}, (blue upright triangle) 7.73×10^{-5}, (dark blue downwards triangle) 1.08×10^{-4}, (black rhombus) 1.54×10^{-4}. Dots are experimental values, and solid lines represent VFT equation approximation (eq 16).

Table 5. Concentration Dependencies of Specific and Molar Electrical Conductivities, Degree of Dissociation and pK_D for C_{60}-Met Aqueous Solutions at T = 298.15 K[ab]

$x_{C_{60}-Met}$	κ/mS·cm^{-1}	λ/S·m^2·mol^{-1}	α	pK_D
0	–	0.68 ± 0.02*	1.000	4.6 ± 0.2*
7.73×10^{-7}	0.023	0.511	0.552	4.5 ± 0.2
1.55×10^{-6}	0.030	0.340	0.367	4.7 ± 0.2
3.09×10^{-6}	0.049	0.287	0.310	4.6 ± 0.2
7.73×10^{-6}	0.114	0.266	0.287	4.3 ± 0.1
1.55×10^{-5}	0.214	0.245	0.270	4.1 ± 0.1
2.32×10^{-5}	0.310	0.240	0.260	3.9 ± 0.1
3.09×10^{-5}	0.391	0.230	0.250	3.9 ± 0.1
3.86×10^{-5}	0.481	0.224	0.242	3.8 ± 0.1

[a]Combined expanded uncertainty is $u_c(\kappa)$ = 0.01 mS·cm^{-1} for T = 298.15 K (0.95 level of confidence). [b]obtained by extrapolation.

Table 6. Values of pK_D for Different C_{60} Fullerene Adducts with Amino Acids at T = 298.15 K

Adduct	pK_D (adduct)	pK_D (amino acid α-COOH)
C_{60}-Arg ($C_{60}(C_6H_{13}N_4O_2)_8H_8$)	7.2[35]	2.2[58]
C_{60}-Thr ($C_{60}(C_4H_9NO_3)_2$)	4.7[36]	2.1[58]
C_{60}-Lys ($C_{60}(C_6H_{14}N_2O_2)_2$)	3.7[32]	2.2[58]

$$V_{C_{60}-Met} = \bar{V} - x_{H_2O}(\partial\bar{V}/\partial x_{H_2O})_{T,P} \quad (3)$$

where x_i is the mole fraction of the *ith* component of the solution. The derivatives $(\partial V/\partial x_{C_{60}-Met})_{T,P}$ and $(\partial V/\partial x_{H_2O})_{T,P}$ were calculated numerically. The concentration dependences of the partial molar volumes of the solution are presented in Figures S7 and S8. As can be seen from Figure S8, the partial molar volumes of C_{60}-Met in aqueous solutions at low concentrations are characterized by negative absolute values (from −100 to −50 cm^3·mol^{-1}). The results are consistent with previously obtained data for other water-soluble C_{60} adducts with amino acids C_{60}-Gly,[41] C_{60}-Arg,[35] C_{60}-Thr,[36] C_{60}-Lys,[32] as well as carboxylated fullerene $C_{60}[C(COOH)_2]_3$[51] and polyhydroxylated fullerenes $C_{60}(OH)_{22-24}$ and $C_{70}(OH)_{12}$.[44,47]

The partial molar volume of C_{60}–Met ($V_{C_{60}-Met}$) is the isothermal–isobaric derivative of the volume of the solution with respect to the number of moles of C_{60}-Met at a constant number of moles of water. Unlike the average molar volume of the solution, it can have an arbitrary sign, in particular, be negative, which indicates strong compaction and structuring of the solution (probably due to the formation of hydrogen bonds) when adding the first portions of C_{60}-Met (up to $x_{C_{60}-Met} = 7.73 \times 10^{-7}$). This fact indirectly indicates that the state of C_{60}-Met molecules in liquid solution (in first-order associates) and in solid C_{60}-Met differs sharply from each other. Further increases in the concentration of C_{60}-Met ($x_{C_{60}-Met} = 1.55 \times 10^{-5}$) lead to the formation of third-order associates (Figure S8), and the partial molar volume becomes positive and weakly dependent on the concentration (≈500 cm^3·mol^{-1}), which is consistent with the average molar volume of solid C_{60}-Met.

3.1.2. Refraction of Aqueous Solutions of C_{60}–Met. Table 3 presents the refractive indexes of C_{60}–Met aqueous solutions at different concentrations (T = 293.15 K).

The concentration dependences of the specific (r) and molar (R) refractions of C_{60}-Met solutions at 293.15 K were determined using the Lorentz–Lorenz equation:

$$r = \frac{n_D^2 - 1}{(n_D^2 + 2)\cdot\rho} \quad (4)$$

$$R = \frac{(n_D^2 - 1)\cdot\bar{M}}{(n_D^2 + 2)\cdot\rho} \quad (5)$$

$$\bar{M} = M_{H_2O}\cdot x_{H_2O} + M_{C_{60}-Met}\cdot x_{C_{60}-Met} \quad (6)$$

The concentration dependences of r and R for aqueous solutions are presented in Table 3. Obviously, the r and R values of C_{60}-Met can be calculated using the refraction of water:

$$r = (r_{H_2O}\cdot\omega_{H_2O} + r_{C_{60}-Met}\cdot\omega_{C_{60}-Met})\cdot(1/100) \quad (7)$$

$$R = R_{H_2O}\cdot x_{H_2O} + R_{C_{60}-Met}\cdot x_{C_{60}-Met} \quad (8)$$

For the C_{60}-Met adduct, the values of the molar ($R_{C_{60}-Met}$) and specific ($r_{C_{60}-Met}$) refractions are $(3.0 \pm 0.2)\cdot10^{-4}$ m^3·mol^{-1} and $(2.6 \pm 0.3)\cdot10^{-4}$ m^3·kg^{-1}, respectively. Due to the low accuracy of the refraction data at $x_{C_{60}-Met} < 7.73 \times 10^{-7}$ these values were not used.

The $R_{C_{60}-Met}$ values were additionally calculated using the Eisenlohr additivity rule at different spectral lines (Hα [λ = 658.3 nm] and Hβ [λ = 436.1 nm]).

$R_{C_{60}-Met} \approx 60R_C + 3\cdot(5R_C + 11R_H + R_{N(-NH-)} + R_{O(-C=O)} + R_{O(-OH)} + R_{S(-S-)} + 33R \approx 60 \times 2.418 + 3\cdot(5 \times 2.418 + 11 \times 1.10 + 2.502 + 2.211 + 1.525 + 8.0) + 33 \times 1.733 \approx 317.55 \pm 5$ cm^3·mol^{-1} ≈ $(3.18 \pm 0.05)\cdot10^{-4}$ m^3·mol^{-1}

The specific refractions of C_{60}-Met were calculated according to eq 9:

$$r_{C_{60}-Met} \approx R_{C_{60}-Met}/M_{C_{60}-Met} \approx (2.72 \pm 0.02)\cdot10^{-4}\ \text{m}^3\cdot\text{kg}^{-1} \quad (9)$$

https://doi.org/10.1021/acs.jced.5c00146
J. Chem. Eng. Data XXXX, XXX, XXX–XXX

Table 7. Temperature (T) and Concentration (C) Dependences of the Speed of Sound (c) of Aqueous Solutions of C_{60}-Met at p = 0.1 MPa[a]

C_m/mol·kg^{-1}	c/m·s^{-1}									
	T/K									
	278.15	283.15	288.15	293.15	298.15	303.15	308.15	313.15	318.15	323.15
8.57×10^{-6}	1427.0	1447.6	1466.1	1482.3	1496.6	1509.0	1519.7	1529.1	1536.7	1542.9
4.3×10^{-5}	1427.0	1447.6	1466.1	1482.3	1496.6	1509.0	1519.8	1529.1	1536.7	1542.9
8.6×10^{-5}	1427.0	1447.5	1466.1	1482.3	1496.5	1508.9	1519.7	1528.8	1536.6	1542.9
2.14×10^{-4}	1427.0	1447.6	1466.1	1482.3	1496.6	1509.0	1519.7	1529.0	1536.7	1542.9
4.3×10^{-4}	1427.0	1447.7	1466.1	1482.3	1496.6	1509.1	1519.8	1529.1	1536.7	1542.9
8.6×10^{-4}	1426.8	1447.6	1466.2	1482.5	1496.7	1509.1	1519.8	1528.9	1536.7	1543.0
2.1×10^{-3}	1427.4	1448.0	1466.5	1482.6	1496.9	1509.3	1520.0	1529.3	1536.9	1543.1
4.32×10^{-3}	1428.2	1448.8	1467.2	1483.4	1497.6	1510.0	1520.7	1530.0	1537.6	1543.8
8.64×10^{-3}	1429.2	1449.6	1468.0	1484.1	1498.3	1510.7	1521.4	1530.2	1538.2	1544.3

[a][a]Standard uncertainties $u(T)$ = 0.01 K and $u(P)$ = 10 kPa. Combined expanded uncertainty for u is $U_c(c)$ = 0.5 m·s^{-1} (0.95 level of confidence).

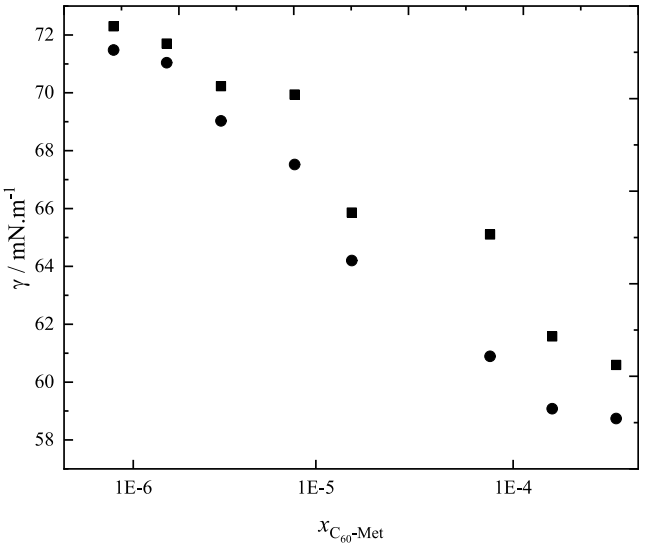

Figure 2. Concentration dependences ($x_{C_{60}-Met}$) of surface tension (γ) of C_{60}-Met aqueous solutions at T = (■) 298.15 K and (●) 303.15 K, x is the mole fraction of C_{60}-Met.

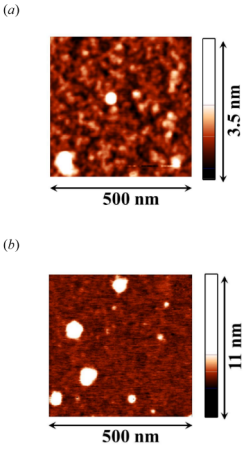

Figure 3. AFM microphotographs of surface films from C_{60}-Met solutions at $x_{C_{60}-Met}$= 7.73× 10^{-6} (a) and $x_{C_{60}-Met}$= 7.73 × 10^{-5} (b).

Thus, there is good agreement between the values calculated using the Eisenlohr additivity rule and the experimental data on the refraction indexes.

3.1.3. Viscosity of Aqueous Solutions of C_{60}-Met. Table 4 and Figure S9 present the $T-x$ dependences of the dynamic viscosity of C_{60}-Met at T = 293.15 to 333.15 K: the dynamic viscosity η increases with the rise in C_{60}-Met concentration.

The kinematic viscosities (η_k) were determined according to the following equation:

$$\eta_k = \eta/\rho \tag{10}$$

where η is the dynamic viscosity and ρ is the density of C_{60}-Met aqueous solutions.

The values of viscous flow activationΔH^*, ΔS^*, and ΔG^* for C_{60}-Met aqueous solutions were calculated using Eyring transition state theory, according to the following equations:[43]

$$\Delta G^* = RT \ln \frac{\eta V}{hN_A} \tag{11}$$

$$\Delta H^* = -RT^2 \frac{\partial}{\partial T}\left(\ln \frac{\eta V}{hN_A}\right) \tag{12}$$

$$\Delta S^* = -\frac{\Delta G^* - \Delta H^*}{T} \tag{13}$$

The activation energy of viscous flow (E_a), the entropic factor (A_s), and the activation temperature (T_A) were determined using eqs 14and 15 (see Table S2):

$$\ln \eta = \ln A_S + \frac{E_a}{R}\frac{1}{T} \tag{14}$$

$$T_A = \frac{-E_a}{R \ln A_S} \tag{15}$$

Isoconcentrates of dynamic viscosity in the temperature range T = 293.15−333.15 K (Figure 1) were determined using the three-parameter Vogel−Fulcher−Tammann (VFT) equation (see Table S3):

$$\lg \eta\ (T) = \lg \eta_0 + A/(T - B) \tag{16}$$

where η_0, A, and B are adjustable parameters.

The values of the adjustable parameters for the VFT equation, as well as the AAD and SD values, are presented in Table S3.

3.1.4. Electrical Conductivity of Aqueous Solutions of C_{60}−Met. Specific (κ) and molar (λ) electrical conductivities of C_{60}−Met aqueous solutions at 298.15 K were calculated according to the following equations:

https://doi.org/10.1021/acs.jced.5c00146
J. Chem. Eng. Data XXXX, XXX, XXX−XXX

Table 8. Sizes of C_{60}-Met Associates in Water at 298.15 K[ab]

$x_{C_{60}-Met}$	δ_0/nm	δ_I /nm	δ_{II} /nm	δ_{III} /μm	$N_{0\rightarrow1}$	$N_{0\rightarrow2}$	$N_{0\rightarrow3}$	ζ_I, MB	ζ_{II}, MB	ζ_{III}, MB
0	2	—	—	—	—	—	—	—	—	
1.55×10^{-5}	—	30−50	—	—	2×10^3−8×10^3	—	—	−35	—	
1.54×10^{-4}	—	30−50	—	—	2×10^3−8×10^3	—	—	−33		
7.72×10^{-4}	—	30−50	100−400	—	2×10^3−8×10^3	$6.5{\cdot}10^4$−$4{\cdot}2 \times 10^6$	—	−30	−40	
1.54×10^{-3}	—	—	100−400	—	—	6.5×10^4−$4{\cdot}2 \times 10^6$	—	—	−37	
3.85×10^{-3}	—	—	100−400	—	—	6.5×10^4−4.2×10^6	—	—	−35	
1.52×10^{-2}	—	—	100−400	1−2	—	6.5×10^4−4.2×10^6	6.5×10^7−5.2×10^8	—	−33	−56
3.72×10^{-2}	—	—	100−400	1−2	—	6.5×10^4−4.2×10^6	6.5×10^7−5.2×10^8	—	−30	−53
7.17×10^{-2}	—	—	100−400	1−2	—	6.5×10^4−4.2×10^6	6.5×10^7−5.2×10^8	—	−27	−49

[a]$N_{0\rightarrow i}$ are the Values of the Average Number of Monomeric Molecules in an i-th Order Associates*; δ_0, δ_i are the Average Diameters of Monomeric Molecules and Associates of the i-th Order; ζ_i is ζ-Potential of the i-th Order Associates. [b]* $N_{0\rightarrow i} = (\frac{\delta_i}{\delta_0})^3 \cdot K_{pack}$, K_{pack} is the packing coefficient in the case of "small spheres packed into a large one" or, equivalently, the packing factor of a sphere into an equidimensional cube: $K_{pack} = \pi/6 \approx 0.52$.

$$\kappa = 1/\rho \tag{17}$$

where ρ is the specific resistance,

$$\lambda = (1000{\cdot}\kappa)/C_M \tag{18}$$

where C_M is the molarity of the solution.

The data on concentration dependencies of specific and molar electrical conductivities at T = 298.15 K are summarized in Table 5.

The analysis of the obtained data shows an increase in specific electrical conductivity and a decrease in molar electrical conductivity with the increase of C_{60}-Met concentration.

Molar electrical conductivity in infinitely dilute solutions (λ_o) was calculated by the extrapolation of $\lambda(\sqrt{C_M})$ to $\sqrt{C_M} = 0$ according to the Kohlrausch equation (eq 19):

$$\lambda = \lambda_o - A{\cdot}\sqrt{C_M} \tag{19}$$

where A is an empirical value that depends on the nature of the electrolyte and solvent, as well as temperature and pressure.

The degree of dissociation (α) and dissociation constant (K_D) of C_{60}−Met in aqueous solutions were determined by eqs 20and 21, assuming a proton dissociation mechanism ($C_{60}(C_4H_{10}NSCOOH)_3 \rightleftarrows C_{60}(C_4H_{10}NSCOOH)_2 C_4H_{10}NSCOO^- + H^+$):

$$\alpha = \lambda/\lambda_o \tag{20}$$

$$K_D = \frac{C_M{\cdot}\alpha^2}{(1-\alpha)} \tag{21}$$

The calculated values of α (Figure S10) and K_D are presented in Table 5 reveal that C_{60}−Met is a weak electrolyte.

The increase of the degree of dissociation (α) upon dilution of the solution from ≈0.242 to 1.00 is quite natural; it is observed for all aqueous solutions of electrolytes when the characteristics of dissociation are determined by the electrical conductivity method. A similar tendency, in particular, is observed for all previously studied adducts of light fullerenes with amino acids.[45,52,53] This fact is due to the electrophoretic and relaxation effects increasing with the concentration of the electrolyte, which limit the charge transfer and mobility of ions. In principle, the decrease in the strength of the electrolyte with increasing concentration in highly polar solvents (water) is a well-known fact. It should also be noted that the obtained values of the molar conductivity in infinitely dilute solutions (λ_o (C_{60}-Met) ≈ 0.68 ± 0.02 $S{\cdot}m^2{\cdot}mol^{-1}$) is in a good agreement with triple molar conductivity of a proton in aqueous solutions (λ_o = 0.225 × 3 = 0.675 $S{\cdot}m^2{\cdot}mol^{-1}$).[54] This fact allows us to propose that the dissociation of C_{60}-Met in infinitely dilute solutions is accompanied by the release of three hydrated protons.

The thermodynamic dissociation constant (K_D^{therm}) was calculated by extrapolating K_D values to the region of an infinitely dilute solution:

$$K_D^{therm} = \lim_{C_M \rightarrow 0} K_D \tag{22}$$

Considering those aqueous solutions of C_{60}-Met that form associates, the K_D values are conditional. For the C_{60}-Met adduct, the value of pK_D^{therm} is 4.6; for comparison, the $pK_{D(-COOH)}$ in Met is equal to 2.1. Thus, attaching an amino acid to the C_{60} core leads to a decrease in the acidity of the carboxyl group. The obtained result is consistent with the fact that fullerenes can exhibit electron-donor properties.[55]

The monotonic decrease in pK_D (from ≈ 4.6 to 3.8) with increasing concentration is quite difficult to explain (see Table 5). The calculation of pK_D was carried out using Ostwald's dilution law (eq 21), without taking into account the activity coefficients of the ion-molecular forms. Moreover, the charge carriers in the system under study change depending on the concentration: monomeric forms (which were not detected in the studied concentration range) and associates of the first, second, and third orders. The activity coefficients of the monomers within such associates are not available, but from general considerations, in strongly associated concentrated solutions of electrolytes, large (sometimes extreme) positive deviations from ideality are observed using asymmetric normalization of excess functions. For example, in concentrated aqueous solutions of $(UO_2)Cl_2$, the values of the average ionic activity coefficients are $\gamma \pm \approx 2000 - 3000$ rel. units.[56] Taking into account the activity coefficients of globally associated C_{60}-Met should significantly reduce the values of thermodynamic dissociation constants with increasing concentration and correct the calculation accordingly The pK_D^{therm} value for C_{60}-Met is equal to 4.6, while the pK_D value of the carboxyl group in Met is equal to 2.1.[57] According to the classical Lewis acid−base theory, electron-donating substituents reduce the strength of acids and increase the strength of bases, and conversely, electron-withdrawing substituents increase the strength of acids and reduce the strength of bases. Thus, the fullerene core C_{60} is an electron-donating ligand for Met. Comparing the pK_D values for C_{60}-Met with the data obtained for C_{60}-Arg, C_{60}-Lys, and C_{60}-Thr (fullerene adducts of C_{60} with L-arginine, L-lysine, and L-threonine, respectively), it can be concluded that the same

https://doi.org/10.1021/acs.jced.5c00146
J. Chem. Eng. Data XXXX, XXX, XXX−XXX

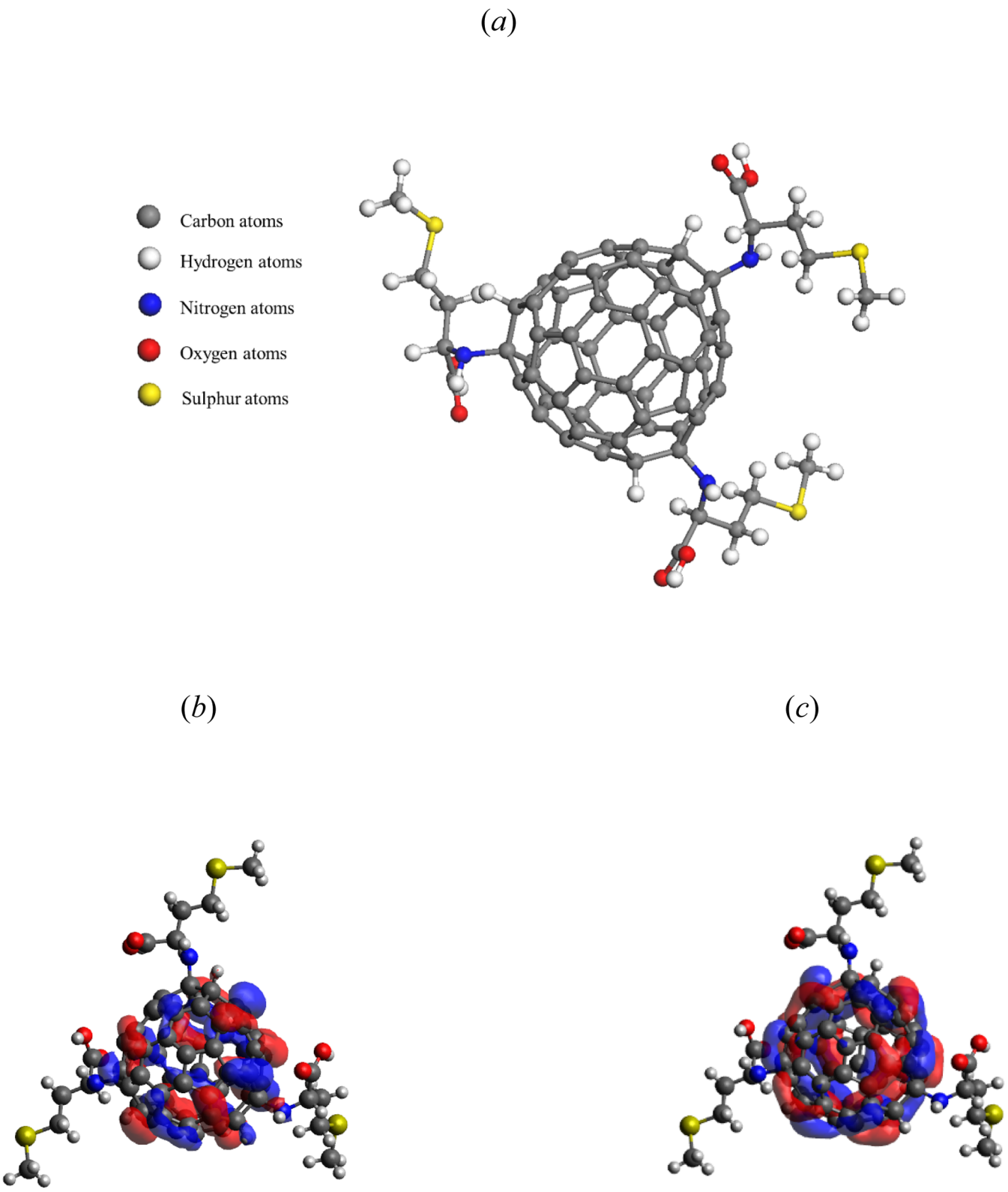

Figure 4. Structure of C_{60}-Met isomer (*a*) and HOMO (*b*) and LUMO (*c*) visualization.

tendency of increasing pK_D of C_{60} fullerene adducts was observed (Table 6).

3.1.5. Speed of Sound in Aqueous Solutions of C_{60}-Met. Concentration and temperature dependencies of the speed of sound (c) and isentropic compressibility (κ_S) of C_{60}-Met solutions are presented in Figure S11 and Table 7. κ_S was determined according to the Laplace equation:

$$\kappa_S = \rho^{-1} \cdot c^{-2} \tag{23}$$

where ρ is the density of C_{60}-Met aqueous solution.

https://doi.org/10.1021/acs.jced.5c00146
J. Chem. Eng. Data XXXX, XXX, XXX−XXX

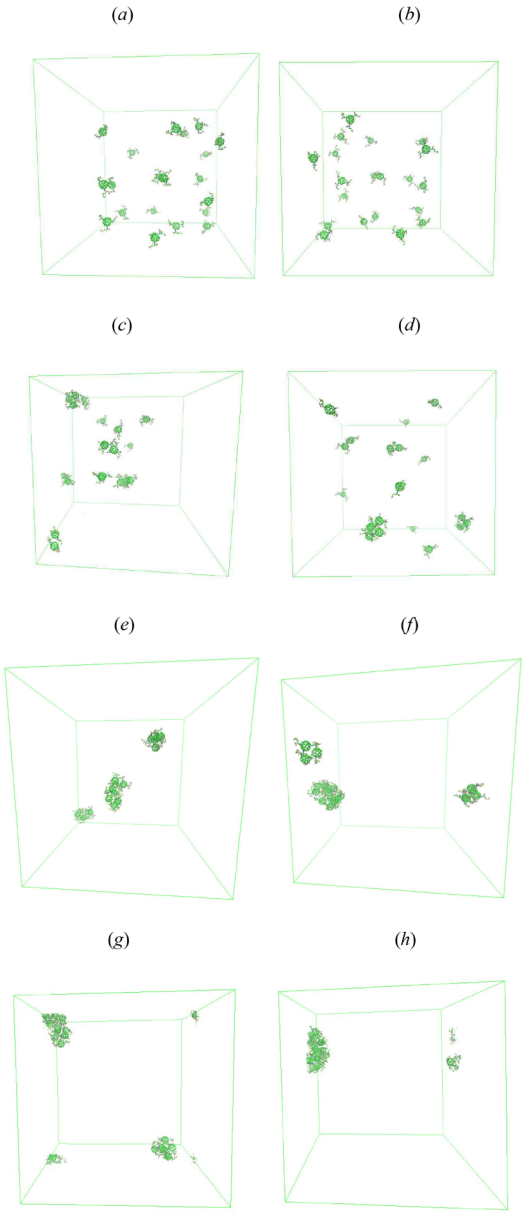

Figure 5. Visualization of C_{60}-Met molecular dynamics: the initial arrangement of C_{60}-Met in cells with water (*a*) and in isotonic saline (*b*); association of C_{60}-Met in water (*c*) and in isotonic saline (*d*) after 10 ns; association of C_{60}-Met in water (*e*) and in isotonic saline (*f*) after 100 ns; association of C_{60}-Met in water (*g*) and in isotonic saline (*h*) after 400 ns.

The values of isentropic compressibilities were used for calculating the apparent specific isentropic compressibility (κ_S,ϕ) according to eq 24:

$$\kappa_{S,\phi} = \frac{\kappa_S(1 + m_{C_{60}-\mathrm{Met}})}{\rho m_{C_{60}-\mathrm{Met}}} - \frac{\kappa_{S0}}{\rho_0 m_{C_{60}-\mathrm{Met}}} \quad (24)$$

where $m_{C_{60}-\mathrm{Met}}$ is the molality of the solution, κ_{S0} is the isentropic compressibility of water, and ρ_0 is the density of water.

The concentration dependencies of κ_S,ϕ in C_{60}-Met aqueous solutions at various temperatures are presented in Figure S12. The negative values of κ_S,ϕ demonstrate that water molecules located near the C_{60}-Met nanoparticles have greater compression resistance than bulk molecules of water. The obtained result

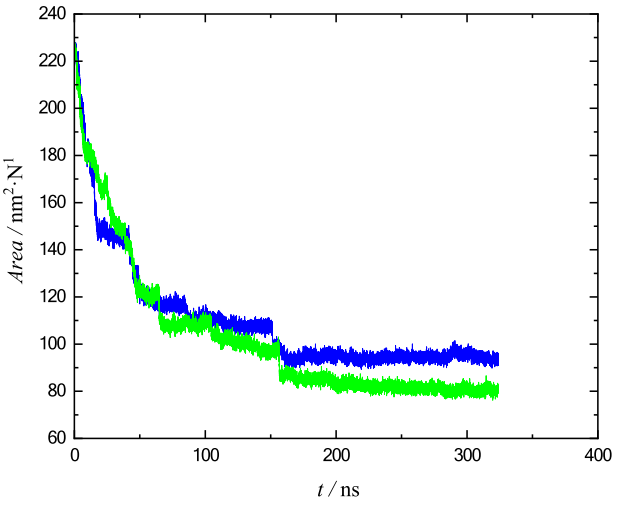

Figure 6. Kinetics of change in solvent-accessible surface area of C_{60}-Met molecule associates in water (shown in blue) and isotonic saline (shown in green). *N* is the number of C_{60}-Met.

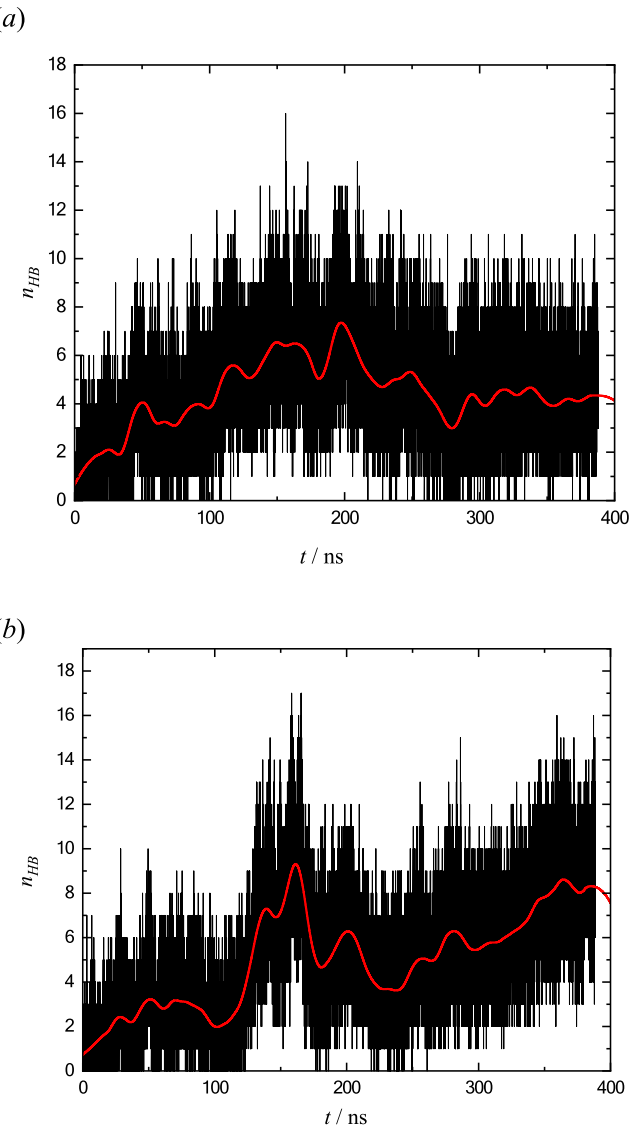

Figure 7. The number of hydrogen bonds formed between C_{60}-Met in water (*a*) and isotonic saline (*b*) during simulation.

https://doi.org/10.1021/acs.jced.5c00146
J. Chem. Eng. Data XXXX, XXX, XXX−XXX

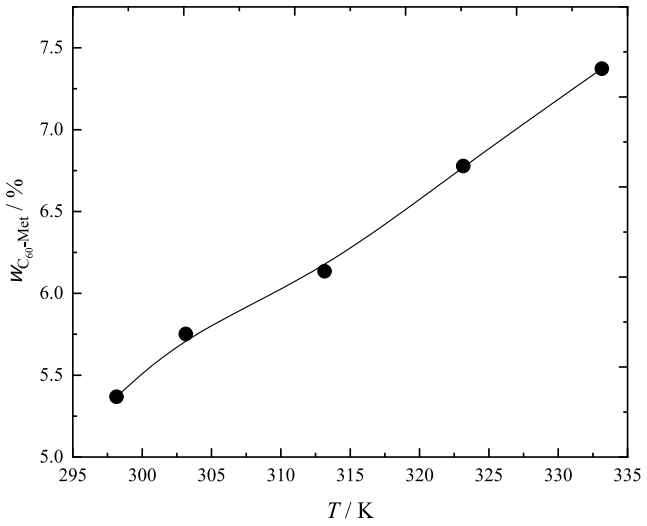

Figure 8. Solubility in the binary system C_{60}-Met−H_2O system at 298.15 to 333.15 K. ω is the mass fraction of C_{60}-Met and T is the absolute temperature (black dots represent experimental data).

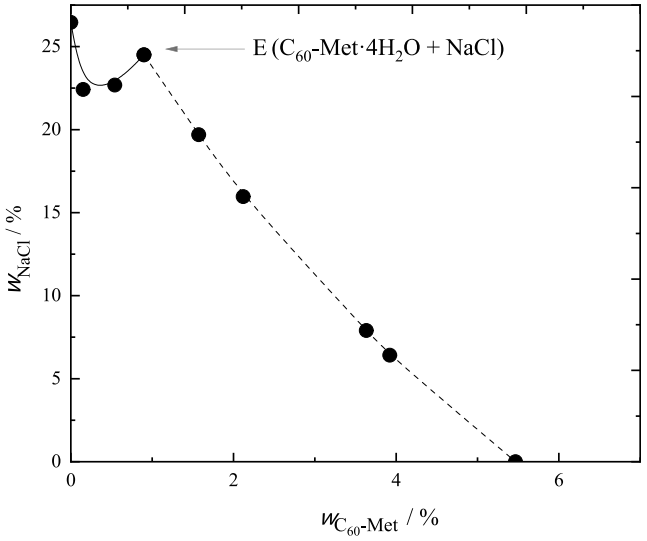

Figure 9. Solubility in the C_{60}-Met−NaCl−H_2O system at 298.15 K (the dashed line corresponds to the crystallization of C_{60}-Met·4H_2O and the solid line to the crystallization of NaCl; ω is the mass fraction.

is in agreement with the fact of condensing C_{60}-Met aqueous solutions at low concentrations (see Section 3.1.1). Figure S12 shows that κ_S,ϕ rises with increasing C_{60}-Met concentration; at the same time, temperature has virtually no effect on the concentration dependence of κ_S,ϕ. The obtained results correspond to the data obtained earlier for C_{60}-Arg,[35] C_{60}-Thr,[36] C_{60}-Lys,[32] and $C_{60}[C(COOH)_2]_3$.[51]

3.1.6. Surface Properties of C_{60}-Met Water Solutions. Plate mass values based on electronic microbalance readings were used to calculate the surface tension (eq 25):

$$\gamma = mk \tag{25}$$

where m is the mass of the plate, and $\kappa = \gamma(H_2O)/m$ is a constant depending on the characteristics of the plate, the value of which was determined from calibration experiments with water. Figure S13 presents the kinetic dependencies of γ at different concentrations of C_{60}-Met aqueous solutions. The obtained data show that (*i*) the surface tension of C_{60}-Met aqueous solutions depends on concentration, (*ii*) the C_{60}-Met−H_2O system needs about 20 to 500 min to reach equilibrium, depending on the concentration of C_{60}-Met in the solution (Figure S13). Figure 2 presents the static surface tension isotherms for C_{60}-Met aqueous solution at T = 298.15 and 303.15 K. The surface tension values were obtained from the kinetic dependences (Figure S13) after the equilibrium was reached.

As can be seen, C_{60}-Met reduces *the* $\gamma\Delta\Delta$ value down to 60.6 mN·m^{-1} at 298.15 K and $x_{C_{60}-Met} = 3.08 \times 10^{-4}$. In our research group, similar surface tension isotherms were obtained earlier for binary systems containing a C_{70} adduct with L-threonine ($C_{70}(C_4H_9NO_2)_2$)[39]—63.5 mN·m^{-1} at x = 5.02 × 10^{-5} and carboxylated fullerene ($C_{60}[C(COOH)_2]_3$)[43]—37 mN·m^{-1} at x = 3.51 × 10^{-4}. From the comparison of the presented values, it follows that C_{60}-Met is a less surface-active substance compared to the surface activity of carboxylated fullerene, but more surface-active compared to the adduct of fullerene C_{70} with L-threonine, which is determined by the structural features of the fullerene adducts. For the investigation of the surface morphology in C_{60}-Met−H_2O binary system, the adsorption films were obtained at $x_{C_{60}-Met} = 7.73 \times 10^{-6}$ and 7.73×10^{-5} and studied using AFM. Figure 3 shows that the surface layer is microheterogeneous due to the adsorption of aggregates from the bulk phase.

As can be seen from Figure 3 in the surface layer at $x_{C_{60}-Met}$ = 7.73 × 10^{-6} associates with sizes of 30 to 50 nm are predominantly present, and at $x_{C_{60}-Met}$ = 7.73× 10^{-5} associates have linear dimensions of about 100 nm. Table 8 and Figure S14 present the concentration dependence of associates' size distribution and ζ-potentials of C_{60}-Met aqueous solutions.

It is clearly seen that the solutions of C_{60}-Met are associated (see Figure 3); the size of the associates depends on concentration and varies from tens to thousands of nm. At the same time, the ζ-potentials calculated using the Helmholtz−Smoluchowski equation demonstrate aggregative stability.[59]

3.1.7. Molecular Dynamics Modeling. The isomer of C_{60}-Met with a maximally distant location of amino acid residues was chosen for computer modeling (see Figure 4a). In this case, the association of C_{60}-Met in solution is possible through hydrophobic interactions as well as due to the formation of hydrogen bonds between amino acid residues. The calculated HOMO and LUMO energy values for C_{60}-Met were −0.240304 Ha and −0.054095 Ha, respectively. The visualization of these orbitals is presented in Figures 4*b*,*c*.

The results for C_{60}-Met in water and isotonic saline (0.15 M NaCl) at 10, 100, and 400 ns are presented in Figure 5.

Figure 5 shows that C_{60}-Met nanoparticles approach each other quite dynamically: at 10 ns, dimers of C_{60}-Met molecules were formed in both systems (Figure 5*c*,*d*). In contrast to isotonic saline, a more uniform association of C_{60}-Met molecules was observed in water, with the formation of groups containing two or three C_{60}-Met molecules. The analysis of the kinetics of C_{60}-Met association in water and isotonic saline shows that, in the latter, the association is more pronounced. Figure 6 shows the kinetics of C_{60}-Met association in water and isotonic saline.

Literature data on modeling the association of fullerenes and their derivatives is very limited, despite the fact that it forms the basis for understanding the mechanism of this process. At the moment, a number of publications are devoted to the study of the aggregation of individual fullerenes and their derivatives, in which the following systems were investigated: fullerenes with

https://doi.org/10.1021/acs.jced.5c00146
J. Chem. Eng. Data XXXX, XXX, XXX−XXX

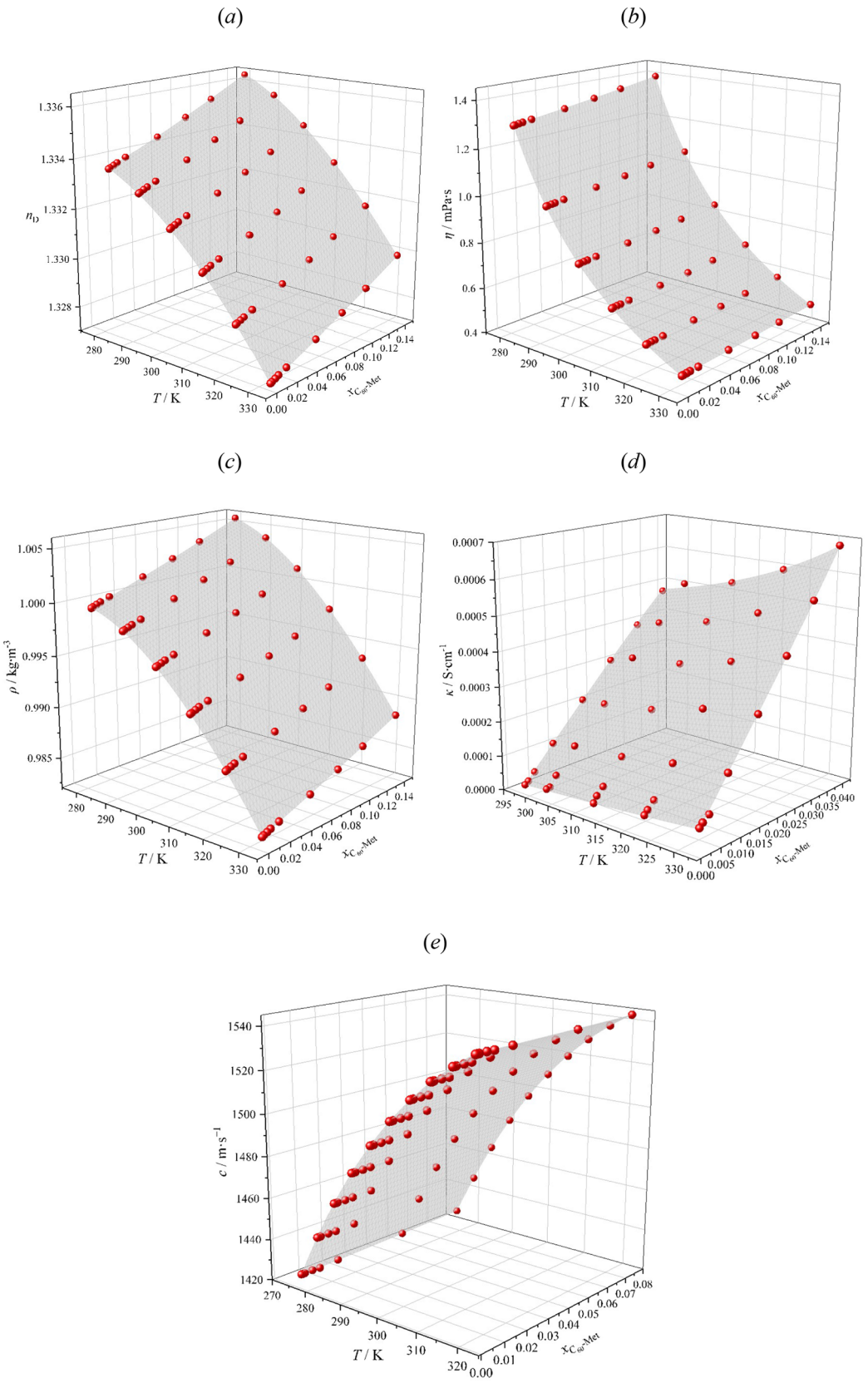

Figure 10. $T-C$ dependences of refraction indexes (a), viscosities (b), densities (c), electrical conductivity (d), and speed of sound (e) of C_{60}-Met aqueous solutions; red spheres: experimental data; surfaces: calculated data.

different numbers of carbon atoms (C_{60}, C_{180}, C_{240}, and C_{540})–water, acetone, and toluene;[60] C_{60}–water and 0.01, 0.1, and 0.4 M aqueous solutions of NaCl;[61] [6,6]-phenyl-C_{61}-butyric acid methyl ester in toluene, indane, toluene–indane mixtures , chlorobenzene, *o*-dichlorobenzene, 1-chloronaphthalene, and 1,8-diiodooctane.[62] The closest to the studied systems are the

https://doi.org/10.1021/acs.jced.5c00146
J. Chem. Eng. Data XXXX, XXX, XXX–XXX

systems of C_{60} adduct with L-arginine ($C_{60}(C_6H_{13}N_4O_2)_8H_8$) in water and in isotonic NaCl solution, in which similar patterns of the association process were obtained,[63] and it was shown that aggregation in isotonic NaCl solution has a more pronounced character.

The higher potential for clustering in isotonic saline is evident from the decrease in the solvent-accessible surface during the simulation compared to the behavior of C_{60}-Met molecules in water (Figure 6). As can be seen, equilibrium in C_{60}-Met−H_2O and C_{60}-Met−isotonic saline systems was reached at about 200 ns from the start of the simulation. Figure 7 presents the number of hydrogen bonds formed between the C_{60}-Met molecules during their association in water and isotonic saline over 400 ns of simulation.

As can be seen from Figure 7*a*, in the case of the water solution of C_{60}-Met the equilibrium in hydrogen bond formation between C_{60}-Met was established at 200 ns. In the case of hydrogen bond formation between C_{60}-Met in isotonic saline (Figure 7*b*), fluctuations with higher amplitude can be seen, which can be connected with the rearrangement of hydrogen bonds inside the C_{60}-Met associate.

3.1.8. Solubility of C_{60}-Met in Water. Solubility in the binary system C_{60}-Met−H_2O in the temperature range T = 298.15 to 333.15 K is presented in Figure 8, from which it follows that (*i*) the solubility curve contains one branch, and an increase in solubility with rising temperature is observed, (*ii*) the equilibrium solid phase in the whole temperature range is the crystal hydrate C_{60}-Met·$4H_2O$, (*iii*) C_{60}-Met is compatible with water, and according to Figure 8 the solubility varies from $x_{C_{60}-Met} = 8.34 \times 10^{-4}$ to 1.14×10^{-3}. Solubility values of the following binary systems were calculated at 298.15 K: C_{60}-Arg-H_2O ($\omega_{C_{60}-Arg} = 0.020$),[35] C_{60}-Thr-H_2O ($\omega_{C_{60}-Thr} = 0.041$),[36] and C_{60}-Lys-H_2O ($\omega_{C_{60}-Lys} = 0.025$)[64] are presented.

Knowing the solubility in the ternary C_{60}-Met−NaCl−H_2O system is important for further biomedical applications of C_{60}-Met. Figure 9 shows that the solubility diagram consists of two branches corresponding to the crystallization of the crystal hydrates of the composition C_{60}-Met·$4H_2O$ and NaCl.

The diagram consists of one invariant point (point E), which corresponds to saturation by C_{60}-Met·$4H_2O$ and NaCl solid phases.

3.1.9. Distribution of C_{60}-Met in the N-Octanol−Water System. The value of $\lg P_{ow}$ of C_{60}-Met is equal to 0.186. The obtained value indicates that C_{60}-Met has similar affinity for the aqueous and *n*-octan-1-ol phases. It is well known that, in the case of $\lg P_{ow} = -1$ to 2, biologically active substances are suitable for oral administration. At a low value of $\lg P_{ow} < -1$, the biologically active substance is poorly absorbed, and, finally, at $\lg P_{ow} > 2$, the substance will be retained in the lipid bilayer.

3.1.10. Correlation Between Physicochemical Properties. For the description of $T-x$ dependencies of density, electrical conductivity, speed of sound, refraction indices, and viscosity, the following equation was applied:

$$P = a + \sum_{i=1}^{4} b_i \cdot T^i + \sum_{j=1}^{4} c_j \cdot C^j \quad (26)$$

where P is a value of the physical property (density, electrical conductivity, speed of sound, refraction indices, and viscosity), a, b_i, c_j are the correlation parameters (see Table S4). The comparisons of experimental and calculated data are presented in Figure 10.

4. CONCLUSIONS

The conducted physicochemical study of C_{60}-Met solutions allows us to conclude that in the region of dilute solutions (up to $x_{C_{60}-Met} = 4.64 \times 10^{-7}$) significant compaction and structuring of the solutions are observed. In the mole fraction range up to 7.73×10^{-5} the solutions were strongly associated, and depending on the concentration, associates of tens, hundreds, and even thousands of nanometers in size were observed. C_{60}-Met solutions are weak electrolytes. The thermodynamic dissociation constant shows that the addition of an amino acid to the C_{60} core leads to a decrease in the acidity of the carboxyl group. C_{60}-Met is a surface-active substance; thus, associates of different sizes were adsorbed in the surface layer depending on the concentration. The C_{60}-Met adduct is compatible with water and aqueous solutions. $\lg P_{ow}$ shows that C_{60}-Met has the same affinity for both phases. Thus, the functionalization of C_{60} does not affect the membranotropic properties. In conclusion, we believe that a comprehensive physicochemical study of fullerene adducts is an important step toward their practical application.

Since the discovery of methods for fullerene preparation, an urgent task has been the synthesis of watersoluble fullerene adducts with a wide range of biological activities: antitumor, antiviral, antimicrobial, antioxidant, neuroprotective, photodynamic, and membranotropic. In addition, they can be used as inhibitors of enzymes and apoptosis, as well as radioprotectors. All this suggests that fullerenes and their derivatives can be the basis for the development of new high-tech medical materials and drugs. Further studies of C_{60}-Met will focus on its mechanisms of action in biological systems: biodegradation, metabolic stability, toxicity, and pharmacokinetics.

■ ASSOCIATED CONTENT

Supporting Information

The Supporting Information is available free of charge at https://pubs.acs.org/doi/10.1021/acs.jced.5c00146.

Information pertaining to the characterization of C_{60}-Met (^{13}C solid-state NMR spectroscopy, IR spectroscopy, elemental analysis, UV/vis spectroscopy, and HPLC); methods and instruments used for identification; data for C_{60}-Met: density, viscosity, refraction indexes, surface tension, size of associates, electrical conductivity, the speed of sound of aqueous solutions; as well as the data of correlation between physicochemical properties (PDF)

■ AUTHOR INFORMATION

Corresponding Authors

Konstantin N. Semenov − *Pavlov First Saint Petersburg State Medical University, Saint Petersburg 197022, Russia; Institute of Chemistry, Saint Petersburg State University, Saint Petersburg 198504, Russia;* orcid.org/0000-0003-2239-2044; Email: knsemenov@gmail.com

Vladimir V. Sharoyko − *Pavlov First Saint Petersburg State Medical University, Saint Petersburg 197022, Russia; Institute of Chemistry, Saint Petersburg State University, Saint Petersburg 198504, Russia*; Email: sharoyko@gmail.com

Authors

Ali Mlhem − *Department of Physical Chemistry, St. Petersburg State Institute of Technology (Technical University), Saint Petersburg 190013, Russia*

Alexander V. Akentiev − *Institute of Chemistry, Saint Petersburg State University, Saint Petersburg 198504, Russia*

https://doi.org/10.1021/acs.jced.5c00146
J. Chem. Eng. Data XXXX, XXX, XXX−XXX

Dmitry A. Nerukh − *Department of Mathematics, Aston University, Birmingham B4 7ET, The United Kingdom;* orcid.org/0000-0001-9005-9919
Natalia V. Petukhova − *Pavlov First Saint Petersburg State Medical University, Saint Petersburg 197022, Russia*
Ilnaz T. Rakipov − *Department of Physical Chemistry, Kazan Federal University, Kazan 420008, Russia*
Kirill V. Timoshchuk − *Pavlov First Saint Petersburg State Medical University, Saint Petersburg 197022, Russia*
Gleb O. Iurev − *Pavlov First Saint Petersburg State Medical University, Saint Petersburg 197022, Russia*
Andrey V. Petrov − *Institute of Chemistry, Saint Petersburg State University, Saint Petersburg 198504, Russia*
Igor V. Murin − *Institute of Chemistry, Saint Petersburg State University, Saint Petersburg 198504, Russia*
Nikolay A. Charykov − *Pavlov First Saint Petersburg State Medical University, Saint Petersburg 197022, Russia; Department of Physical Chemistry, St. Petersburg State Institute of Technology (Technical University), Saint Petersburg 190013, Russia*
Olga S. Vezo − *Centre for Diagnostics of Functional Materials for Medicine, Pharmacology and Nanoelectronics, the Research Park, Saint Petersburg State University, Saint Petersburg 198504, Russia*
Anastasia V. Penkova − *Institute of Chemistry, Saint Petersburg State University, Saint Petersburg 198504, Russia*
Dilafruz K. Kholmurodova − *Scientific and practical center of immunology, Allergology and human genomics at Samarkand State Medical University, Samarkand 140100, Uzbekistan*
Jasur A. Rizaev − *Samarkand State Medical University, Samarkand 140100, Uzbekistan*
Aziz S. Kubaev − *Samarkand State Medical University, Samarkand 140100, Uzbekistan*

Complete contact information is available at: https://pubs.acs.org/10.1021/acs.jced.5c00146

Author Contributions

K.N.S.—Conceptualization, validation, supervision, and project administration. A.M.—Investigation of phase equilibria, conducting physicochemical calculations, and measurement of electrical conductivity of aqueous solutions of fullerene adducts. A.V.A.—Investigation of surface properties. D.A.N.—Investigation of association in aqueous solutions using the molecular dynamics method. N.V.P.—Investigation of association in aqueous solutions using the molecular dynamics method. I.T.R.—Investigation and measurement of temperature and concentration dependencies of the speed of sound. K.V.T.—Investigation of association in aqueous solutions using the molecular dynamics method. G.O.I.—Conducting physicochemical calculations and writing and editing of THE original draft. A.V.P.—Conducting quantum chemical calculations. I.V.M.—Validation and supervision. N.A.C.—Conducting physicochemical calculations. O.S.V.—Measurement of temperature and concentration dependencies of viscosity, density, and refraction. A.V.P.—Conducting physicochemical calculations. D.K.K.—Conducting physicochemical calculations. J.A.R.—Conducting physicochemical calculations. A.S.K.—Conducting physicochemical calculations. V.V.S.—Writing (original draft and editing), project administration, and funding acquisition.

Notes

The authors declare no competing financial interest.

■ ACKNOWLEDGMENTS

The authors acknowledge Saint Petersburg State University for a research grant (102591880). The equipment of the following Resource Centers of the Research Park of Saint Petersburg State University was used: the Computing Center, the Center for Diagnostics of Functional Materials for Medicine, Pharmacology and Nanoelectronics, the Magnetic Resonance Research Center, Center for Chemical Analysis and Materials Research. D. N. acknowledges the use of the HPC Midlands supercomputer funded by EPSRC, grant number EP/P020232/1; access to HPC Call Spring 2021, EPSRC Tier-2 Cirrus Service; and access to the Sulis Tier-2 HPC platform hosted by the Scientific Computing Research Technology Platform at the University of Warwick. Sulis is funded by EPSRC Grant EP/T022108/1 and the HPC Midlands+ consortium. The collaboration was supported by the program H2020-MSCA-RISE-2018, project AMR-TB, Grant ID: 823922.

■ REFERENCES

(1) Semenov, K. N.; Charykov, N. A.; Postnov, V. N.; Sharoyko, V. V.; Vorotyntsev, I. V.; Galagudza, M. M.; Murin, I. V. Fullerenols: Physicochemical Properties and Applications. *Prog. Solid State Chem.* **2016**, *44* (2), 59−74.
(2) Semenov, K. N.; Andrusenko, E. V.; Charykov, N. A.; Litasova, E. V.; Panova, G. G.; Penkova, A. V.; Murin, I. V.; Piotrovskiy, L. B. Carboxylated Fullerenes: Physico-Chemical Properties and Potential Applications. *Prog. Solid State Chem.* **2017**, *47*−*48*, 19−36.
(3) Bezmel'nitsyn, V. N.; Eletskii, A. V.; Okun', M. V. Fullerenes in Solutions. *Physics-Uspekhi* **1998**, *41* (11), 1091−1114.
(4) Bagchi, D.; Bagchi, M.; Moriyama, H.; Shahidi, F.. *Bio-Nanotechnology: A Revolution in Food, Biomedical and Health Sciences*; John Wiley & Sons, Ltd., 2013: DOI:
(5) Sharoyko, V. V.; Ageev, S. V.; Podolsky, N. E.; Petrov, A. V.; Litasova, E. V.; Vlasov, T. D.; Vasina, L. V.; Murin, I. V.; Piotrovskiy, L. B.; Semenov, K. N. Biologically Active Water-Soluble Fullerene Adducts: Das Glasperlenspiel (by H. Hesse)? *J. Mol. Liq.* **2021**, *323*, 114990.
(6) Pochkaeva, E. I.; Podolsky, N. E.; Zakusilo, D. N.; Petrov, A. V.; Charykov, N. A.; Vlasov, T. D.; Penkova, A. V.; Vasina, L. V.; Murin, I. V.; Sharoyko, V. V.; et al. Fullerene Derivatives with Amino Acids, Peptides and Proteins: from Synthesis to Biomedical Application. *Prog. Solid State Chem.* **2020**, *57*, 100255.
(7) Matsubayashi, K.; Kokubo, K.; Tategaki, H.; Kawahama, S.; Oshima, T. One-step Synthesis of Water-soluble Fullerenols Bearing Nitrogen-containing Substituents. *Fullerenes, Nanotubes Carbon Nanostruct.* **2009**, *17* (4), 440−456.
(8) Khan, F. I.; Aggarwal, A.; Upadhyay, N.; Vishnurao, S. G.; Jha, N. Fullerenes in Dentistry: A Review on Unlocking Their Therapeutic Potential in Oral Medicine. *J. Oral Med. Oral Surg Oral Pathol Oral Radiol.* **2024**, *10* (3), 149−153.
(9) Kulkarni, S.; Chaudhari, S. B.; Chikkamath, S. S.; Kurale, R. S.; Thopate, T. S.; Praveenkumar, S.; Ghotekar, S.; Patil, P.; Kumar, D. Potential Applications of Fullerenes in Drug Delivery and Medical Advances. *Inorg. Chem. Commun.* **2025**, *173*, 113829.
(10) Pesado-Gómez, C.; Serrano-García, J. S.; Amaya-Flórez, A.; Pesado-Gómez, G.; Soto-Contreras, A.; Morales-Morales, D.; Colorado-Peralta, R. Fullerenes: Historical Background, Novel Biological Activities versus Possible Health Risks. *Coord. Chem. Rev.* **2024**, *501*, 215550.
(11) Kukalia, O. N.; Meshcheryakov, A. A.; Iurev, G. O.; Andoskin, P. A.; Semenov, K. N.; Molchanov, O. E.; Maistrenko, D. N.; Murin, I. V.; Sharoyko, V. V. Prospects for the Application of Water-Soluble Derivatives of Light Fullerenes in Medicine. *Trans Med.* **2024**, *10* (6), 507−521.
(12) Patrick, G. *An Introduction to Medicinal Chemistry*; Oxford University Press, 2017.

(13) Czechtizky, W.; Hamley, P. *Small Molecule Medicinal Chemistry: strategies and Technologies*; Wiley, 2015.
(14) Silverman, R. B.; Holladay, M. W. *The Organic Chemistry of Drug Design and Drug Action*. 3rded.; Elsevier, 2015. DOI: .
(15) Kustov, A. V.; Antonova, O. A.; Smirnova, N. L.; Kladiev, A. A.; Kladiev, A. A.; Kudayarova, T. V.; Gruzdev, M. S.; Berezin, D. B. The Energetics of Solvation and Ion-Ion Interactions in Prospidium Chloride Aqueous Solutions. *J. Mol. Liq.* **2018**, *263*, 49−52.
(16) Akbaş, H.; KaradaĞ, A.; Aydın, A.; Destegül, A.; Kılıç, Z. Synthesis Structural and Thermal Properties of the Hexapyrrolidino-cyclotriphosphazenes-Based Protic Molten Salts: Antiproliferative Effects against HT29, HeLa, and C6 Cancer Cell Lines. *J. Mol. Liq.* **2017**, *230*, 482−495.
(17) Nikolaienko, T. Y. Interaction of Anticancer Drug Doxorubicin with Sodium Oleate Bilayer: Insights from Molecular Dynamics Simulations. *J. Mol. Liq.* **2017**, *235*, 31−43.
(18) Jouyban, A.; Rahimpour, E.; Karimzadeh, Z. A New Correlative Model to Simulate the Solubility of Drugs in Mono-Solvent Systems at Various Temperatures. *J. Mol. Liq.* **2021**, *343*, 117587.
(19) Gurung, J.; Anjudikkal, J.; Pulikkal, A. K. Amphiphilic Drug−Additive Systems in Aqueous and Organic Solvent−Water Mixed Media: A Comprehensive Account on Physicochemical Properties. *J. Mol. Liq.* **2020**, *318*, 114221.
(20) Mondal, M.; Basak, S.; Choudhury, S.; Ghosh, N. N.; Roy, M. N. Investigation of Molecular Interactions Insight into Some Biologically Active Amino Acids and Aqueous Solutions of an Anti-Malarial Drug by Physicochemical and Theoretical Approach. *J. Mol. Liq.* **2021**, *341*, 116933.
(21) Alhumaydhi, F. A.; Aljasir, M. A.; Aljohani, A. S. M.; Alsagaby, S. A.; Alwashmi, A. S. S.; Shahwan, M.; Hassan, M. I.; Islam, A.; Shamsi, A. Probing the Interaction of Memantine, an Important Alzheimer's Drug, with Human Serum Albumin: *In Silico* and *in Vitro* Approach. *J. Mol. Liq.* **2021**, *340*, 116888.
(22) Alam, M. S.; Ashokkumar, B.; Mohammed Siddiq, A. The Density, Dynamic Viscosity and Kinematic Viscosity of Protic Polar Solvents (Pure and Mixed Systems) Studies: A Theoretical Insight of Thermophysical Properties. *J. Mol. Liq.* **2018**, *251*, 458−469.
(23) Mahdi, J. F.; Haque, A. A. J. A.; Farooqui, M. A. N.; Shaikh, Y. H. Effect of Viscosity and Density of Substance on Dielectric Properties of Medicinal Compounds in Solution. *Nano biomed. ENG.* **2020**, *12* (4), 351−357.
(24) Semenov, K. N.; Ageev, S. V.; Kukaliia, O. N.; Murin, I. V.; Petrov, A. V.; Iurev, G. O.; Andoskin, P. A.; Panova, G. G.; Molchanov, O. E.; Maistrenko, D. N.; et al. Application of Carbon Nanostructures in Biomedicine: Realities, Difficulties, Prospects. *Nanotoxicology* **2024**, *18*, 1−33.
(25) Koruga, D.; Stanković, I.; Matija, L.; Kuhn, D.; Christ, B.; Dembski, S.; Jevtić, N.; Janać, J.; Pavlović, V.; De Wever, B. Comparative Studies of the Structural and Physicochemical Properties of the First Fullerene Derivative FD-C_{60} (Fullerenol) and Second Fullerene Derivate SD-C_{60} (3HFWC). *Nanomater* **2024**, *14* (5), 480.
(26) Srivastava, V.; Sinha, S.; Kanaujia, S.; Bartaria, D.; Singh, P. K.; Singh, P. P. Fullerene-Based Photocatalysis as an Eco-Compatible Approach to Photochemical Reactions. *Synth. Commun.* **2025**, *55* (1), 1−18.
(27) Vnukova, N. G.; Isakova, V. G.; Elesina, V. I.; Tomashevich, Y. V.; Churilov, G. N. Study of the Dependence of Hydroxyl Groups Numbers on Treatment Time during the Synthesis of Fullerenols. *Fuller Nanotub Car N* **2025**, 1−6.
(28) Andreeva, N. A.; Chaban, V. V. Electronic and Thermodynamic Properties of the Amino- and Carboxamido-Functionalized C-60-Based Fullerenes: Towards Non-Volatile Carbon Dioxide Scavengers. *J. Chem. Thermodyn* **2018**, *116*, 1−6.
(29) Luzhkov, V. B.; Romanova, V. S.; Kotelnikov, A. I. Quantum Chemical Calculations of the Dissociation Constants PK a for L-Ala-C_{60}H (an Amino Acid Derivative of Fullerene) in Water. *Rus Chem. Bull.* **2014**, *63* (3), 567−571.
(30) Basiuk, V.; Bassiouk, M. Interaction of Short Homopeptides of Glycine and *L* -Alanine with Fullerene C_{60}. *J. Comput. Theor. Nanosci.* **2011**, *8* (2), 243−252.
(31) Timofeeva, G. I.; Romanova, V. S.; Lopanova, L. A. Molecular Characteristics of Water-Soluble Fullerene Derivatives of Amino Acids and Peptides. *Rus Chem. Bull.* **1996**, *45* (4), 834−837.
(32) Semenov, K. N.; Charykov, N. A.; Iurev, G. O.; Ivanova, N. M.; Keskinov, V. A.; Letenko, D. G.; Postnov, V. N.; Sharoyko, V. V.; Kulenova, N. A.; Prikhodko, I. V.; Murin, I. V. Physico-Chemical Properties of the C_{60}-l-Lysine Water Solutions. *J. Mol. Liq.* **2017**, *225*, 767−777.
(33) Noskov, B. A.; Timoshen, K. A.; Akentiev, A. V.; Charykov, N. A.; Loglio, G.; Miller, R.; Semenov, K. N. Dynamic Surface Properties of C_{60}-Arginine and C_{60}-l-Lysine Aqueous Solutions. *Colloids Surf., A* **2017**, *529*, 1−6.
(34) Semenov, K. N.; Meshcheriakov, A. A.; Charykov, N. A.; Dmitrenko, M. E.; Keskinov, V. A.; Murin, I. V.; Panova, G. G.; Sharoyko, V. V.; Kanash, E. V.; Khomyakov, Y. V. Physico-Chemical and Biological Properties of C_{60}-L-Hydroxyproline Water Solutions. *RSC Adv.* **2017**, *7* (25), 15189−15200.
(35) Shestopalova, A. A.; Semenov, K. N.; Charykov, N. A.; Postnov, V. N.; Ivanova, N. M.; Sharoyko, V. V.; Keskinov, V. A.; Letenko, D. G.; Nikitin, V. A.; Klepikov, V. V.; Murin, I. V. Physico-Chemical Properties of the C_{60}-Arginine Water Solutions. *J. Mol. Liq.* **2015**, *211*, 301−307.
(36) Semenov, K. N.; Charykov, N. A.; Meshcheriakov, A. A.; Lahderanta, E.; Chaplygin, A. V.; Anufrikov, Y. A.; Murin, I. V. Physico-Chemical Properties of the C_{60}-L-Threonine Water Solutions. *J. Mol. Liq.* **2017**, *242* (3), 940−950.
(37) Matuzenko, M. Y.; Shestopalova, A. A.; Semenov, K. N.; Charykov, N. A.; Keskinov, V. A. Cryometry and Excess Functions of the Adduct of Light Fullerene C_{60} and Arginine — $C_{60}(C_6H_{12}NaN_4O_2)_8H_8$ Aqueous Solutions. *Nanosyst Phys. Chem. M* **2015**, 715−725.
(38) Danilenko, A. N.; Romanova, V. S.; Kuleshova, E. F.; Parnes, Z. N.; Braudo, E. E. Heat Capacities of Aqueous Solutions of Amino Acid and Dipeptide Derivatives of Fullerene. *Rus Chem. Bull.* **1998**, *47* (11), 2134−2136.
(39) Serebryakov, E. B.; Zakusilo, D. N.; Semenov, K. N.; Charykov, N. A.; Akentiev, A. V.; Noskov, B. A.; Petrov, A. V.; Podolsky, N. E.; Mazur, A. S.; Dul'neva, L. V.; Murin, I. V. Physico-Chemical Properties of C_{70}-L-Threonine Bisadduct ($C_{70}(C_4H_9NO_2)_2$) Aqueous Solutions. *J. Mol. Liq.* **2019**, *279*, 687−699.
(40) Semenov, K. N.; Charykov, N. A.; Meshcheriakov, A. A.; Lahderanta, E.; Chaplygin, A. V.; Anufrikov, Y. A.; Murin, I. V. Physico-Chemical Properties of the C_{60}-l-Threonine Water Solutions. *J. Mol. Liq.* **2017**, *242*, 940−950.
(41) Sharoyko, V. V.; Ageev, S. V.; Meshcheriakov, A. A.; Podolsky, N. E.; Vallejo, J. P.; Lugo, L.; Rakipov, I. T.; Petrov, A. V.; Ivanova, A. V.; Charykov, N. A.; Semenov, K. N. Physicochemical Investigation of Water-Soluble $C_{60}(C_2NH_4O_2)_4H_4$ (C_{60}-Gly) Adduct. *J. Mol. Liq.* **2021**, *344*, 117658.
(42) International Organization for Standardization. *Guide to the expression of uncertainty in measurement (GUM)*; International Organization for Standardization: Switzerland, 2004.
(43) Semenov, K. N.; Charykov, N. A.; Murin, I. V.; Pukharenko, Y. V. Physico-Chemical Properties of the C_{60}-Tris-Malonic Derivative Water Solutions. *J. Mol. Liq.* **2015**, *201*, 50−58.
(44) Semenov, K. N.; Charykov, N. A.; Murin, I. V.; Pukharenko, Y. V. Physico-Chemical Properties of the Fullerenol-70 Water Solutions. *J. Mol. Liq.* **2015**, *202*, 1−8.
(45) Manyakina, O. S.; Semenov, K. N.; Charykov, N. A.; Ivanova, N. M.; Keskinov, V. A.; Sharoyko, V. V.; Letenko, D. G.; Nikitin, V. A.; Klepikov, V. V.; Murin, I. V. Physico-Chemical Properties of the Water-Soluble C_{70}-Tris-Malonic Solutions. *J. Mol. Liq.* **2015**, *211*, 487−493.
(46) Serebryakov, E. B.; Semenov, K. N.; Stepanyuk, I. V.; Charykov, N. A.; Mescheryakov, A. N.; Zhukov, A. N.; Chaplygin, A. V.; Murin, I. V. Physico-Chemical Properties of the C_{70}-l-Lysine Aqueous Solutions. *J. Mol. Liq.* **2018**, *256*, 507−518.

https://doi.org/10.1021/acs.jced.5c00146
J. Chem. Eng. Data XXXX, XXX, XXX−XXX

(47) Podolsky, N. E.; Marcos, M. A.; Cabaleiro, D.; Semenov, K. N.; Lugo, L.; Petrov, A. V.; Charykov, N. A.; Sharoyko, V. V.; Vlasov, T. D.; Murin, I. V. Physico-Chemical Properties of $C_{60}(OH)_{22-24}$ Water Solutions: Density, Viscosity, Refraction Index, Isobaric Heat Capacity and Antioxidant Activity. *J. Mol. Liq.* **2019**, *278*, 342−355.
(48) Sharoyko, V. V.; Ageev, S. V.; Meshcheriakov, A. A.; Akentiev, A. V.; Noskov, B. A.; Rakipov, I. T.; Charykov, N. A.; Kulenova, N. A.; Shaimardanova, B. K.; Podolsky, N. E.; Semenov, K. N. Physicochemical Study of Water-Soluble $C_{60}(OH)_{24}$ Fullerenol. *J. Mol. Liq.* **2020**, *311*, 113360.
(49) Meshcheriakov, A. A.; Iurev, G. O.; Luttsev, M. D.; Podolsky, N. E.; Ageev, S. V.; Petrov, A. V.; Vasina, L. V.; Solovtsova, I. L.; Sharoyko, V. V.; Murin, I. V.; Semenov, K. N. Physicochemical Properties, Biological Activity and Biocompatibility of Water-Soluble C_{60}-Hyp Adduct. *Colloids Surf., B* **2020**, *196*, 111338.
(50) Mikolaichuk, O. V.; Popova, E. A.; Protas, A. V.; Rakipov, T.; Nerukh, D. A.; Petrov, A. V.; Charykov, N. A.; Ageev, V.; Tochilnikov, G. V.; Zmitrichenko, I. G.; et al. A cytostatic drug from the class of triazine derivatives: Its properties in aqueous solutions, cytotoxicity, and therapeutic activity. *J. Mol. Liq.* **2022**, *356*, 119043.
(51) Ageev, S. V.; Iurev, G. O.; Podolsky, N. E.; Rakipov, I. T.; Vasina, L. V.; Noskov, B. A.; Akentiev, A. V.; Charykov, N. A.; Murin, I. V.; Semenov, K. N. D. Speed of Sound, Viscosity, Refractive Index, Surface Tension and Solubility of $C_{60}[C(COOH)_2]_3$. *J. Mol. Liq.* **2019**, *291*, 111256.
(52) Tyurin, D. P.; Semenov, K. N.; Charykov, N. A.; Cherepkova, I. A.; Keskinov, V. A. Dissociation of Fullerenol-70-d in Aqueous Solutions and Their Electric Conductivity. *Russ. J. Phys. Chem. A* **2015**, *89* (5), 771−775.
(53) Semenov, K. N.; Letenko, D. G.; Charykov, N. A.; Nikitin, V. A.; Matuzenko, M. Y.; Keskinov, V. A.; Postnov, V. N.; Kopyrin, A. A. Electrochemical Properties of Aqueous Solutions of Fullerenol-d. *Rus J. Appl. Chem.* **2011**, *84* (1), 79−83.
(54) Ravdel, A.; Ponomareva, A. *Brief Reference Book of Physical and Chemical Quantities Az-Book*. 2009, p 237.
(55) Kano, H.; Matsuo, K.; Hayashi, H.; Kato, K.; Yamakata, A.; Yamada, H.; Aratani, N. Buckyball as an Electron Donor in a Dyad of C_{60} and Xanthene Dye. *Eur. J. Org. Chem.* **2021**, *2021* (23), 3377−3381.
(56) Mikulin, G. I.*Questions of Physical Chemistry of Electrolyte Solutions [Collection of Articles]*; State Research and Design Institute of Basic Chemistry "NIOKhim", 1968.
(57) Kochergina, L. A.; Lytkin, A. I.; Krutova, O. N.; Damrina, K. V. Standard Enthalpies of Formation of L-Cysteine in Aqueous Solution. *Izv. Vyssh. Uchebn. Zaved.* **2013**, *56*, 38−41.
(58) *Amino acid pKa and pKi values*, https://www.iscabiochemicals.com/page/32/amino-acid-pka-and-pki-values.
(59) Delgado, A. V.; González-Caballero, F.; Hunter, R. J.; Koopal, L. K.; Lyklema, J. Measurement and Interpretation of Electrokinetic Phenomena. *J. Colloid Interface Sci.* **2007**, *309* (2), 194−224.
(60) Banerjee, S. Molecular Dynamics Study of Self-Agglomeration of Charged Fullerenes in Solvents. *J. Chem. Phys.* **2013**, *138* (4), 044318.
(61) Mortuza, S. M.; Kariyawasam, L. K.; Banerjee, S. Combined Deterministic-Stochastic Framework for Modeling the Agglomeration of Colloidal Particles. *Phys. Rev. E* **2015**, *92* (1), 013304.
(62) Tummala, N. R.; Sutton, C.; Aziz, S. G.; Toney, M. F.; Risko, C.; Bredas, J.-L. Effect of Solvent Additives on the Solution Aggregation of Phenyl-C_{61} − Butyl Acid Methyl Ester (PCBM). *Chem. Mater* **2015**, *27* (24), 8261−8272.
(63) Sharoyko, V. V.; Kukaliia, O. N.; Darvish, D. M.; Meshcheriakov, A. A.; Iurev, G. O.; Andoskin, P. A.; Penkova, A. V.; Ageev, S. V.; Petukhova, N. V.; Timoshchuk, K. V.; Petrov, A. V.; Akentev, A. V.; Nerukh, D. A.; Mazur, A. S.; Maistrenko, D. N.; Molchanov, O. E.; Murin, I. V.; Semenov, K. N. Protective Action of Water-Soluble Fullerene Adducts on the Example of an Adduct with l-Arginine. *J. Mol. Liq* **2024**, *401*, 124702.
(64) Semenov, K. N.; Kurilenko, A. V.; Charykov, N. A.; Keskinov, V. A.; Vorob'ev, A. L.; Shaimardanov, Z. K.; Kulenova, N. A.; Onalbaeva, Z. S.; Letenko, D. G. S. Thermal Analysis, and Association of the Bis-Adducts of Light C_{60} Fullerene and Amino Acids Lysine, Threonine, and Hydroxyproline in Aqueous Solutions. *Russ. J. Phys. Chem. A* **2019**, *93* (7), 1258−1265.

https://doi.org/10.1021/acs.jced.5c00146
J. Chem. Eng. Data XXXX, XXX, XXX−XXX